

Terahertz emission mechanism of magnesium doped indium nitride

H. Ahn, Y.-J. Yeh, Y.-L. Hong, and S. Gwo

Citation: *Applied Physics Letters* **95**, 232104 (2009); doi: 10.1063/1.3270042

View online: <http://dx.doi.org/10.1063/1.3270042>

View Table of Contents: <http://scitation.aip.org/content/aip/journal/apl/95/23?ver=pdfcov>

Published by the *AIP Publishing*

Articles you may be interested in

[Infrared to vacuum-ultraviolet ellipsometry and optical Hall-effect study of free-charge carrier parameters in Mg-doped InN](#)

J. Appl. Phys. **113**, 013502 (2013); 10.1063/1.4772625

[Properties of In_xGa_{1-x}N films in terahertz range](#)

Appl. Phys. Lett. **100**, 071913 (2012); 10.1063/1.3684836

[Mg-induced terahertz transparency of indium nitride films](#)

Appl. Phys. Lett. **99**, 232117 (2011); 10.1063/1.3669538

[Effect of Mg doping on enhancement of terahertz emission from InN with different lattice polarities](#)

Appl. Phys. Lett. **96**, 061907 (2010); 10.1063/1.3303983

[Terahertz emission from silicon and magnesium doped indium nitride](#)

Appl. Phys. Lett. **93**, 221113 (2008); 10.1063/1.3043450

The advertisement features a dark blue background with a grid of images showing various AFM scan results. The text 'NEW! Asylum Research MFP-3D Infinity™ AFM' is prominently displayed in white and orange. Below it, the tagline 'Unmatched Performance, Versatility and Support' is written in orange. The Oxford Instruments logo, 'The Business of Science®', is in the top right. Four key features are highlighted with corresponding images: 'Stunning high performance' (AFM scan of a surface), 'Simpler than ever to GetStarted™' (AFM scan of a surface), 'Comprehensive tools for nanomechanics' (AFM scan of a surface with circular features), and 'Widest range of accessories for materials science and bioscience' (AFM scan of a surface with rectangular features). An image of the MFP-3D Infinity AFM system is shown in the bottom right corner.

Terahertz emission mechanism of magnesium doped indium nitride

H. Ahn,^{1,a)} Y.-J. Yeh,¹ Y.-L. Hong,² and S. Gwo²

¹Department of Photonics and Institute of Electro-Optical Engineering, National Chiao Tung University, Hsinchu 30010, Taiwan

²Department of Physics, National Tsing Hua University, Hsinchu 30013, Taiwan

(Received 30 May 2009; accepted 10 November 2009; published online 7 December 2009)

We report carrier concentration-dependence of terahertz emission from magnesium doped indium nitride (InN:Mg) films. Near the critical concentration ($n_c \sim 1 \times 10^{18} \text{ cm}^{-3}$), the competition between two emission mechanisms determines the polarity of terahertz emission. InN:Mg with $n > n_c$ exhibits enhanced positive polarity terahertz emission compared to the undoped InN, which is due to the reduced screening of the photo-Dember field. For InN:Mg with $n < n_c$, the polarity of terahertz signal changes to negative, indicating the dominant contribution of the surface electric field due to the large downward surface band bending within the surface layer extending over the optical absorption depth. © 2009 American Institute of Physics. [doi:10.1063/1.3270042]

Recently, research activities in indium nitride (InN) have been dramatically increased due to its potential applications in high-frequency electronic devices, near-infrared optoelectronics, and high-efficiency solar cells. To realize the InN-based optoelectronic devices, it is essential to have the ability to fabricate both *n*-type and *p*-type InN. Due to its high electron affinity, however, *p*-type doping of InN is known to be difficult and the growth and identification of *p*-type InN is one of the main challenges among the InN research community. With a recent report of indirectly observed *p*-type conductivity,¹ it is reasonably accepted that *p*-type InN can be realized by using magnesium (Mg) as an acceptor dopant and recently, a series of works have been reported on the support of proposition that for Mg-doped InN (InN:Mg) film, *p*-type bulk InN:Mg lies under the surface layer composed of a thin surface electron accumulation layer and a rather thicker charge depletion layer.¹⁻⁴

One of the promising applications of InN has been identified to be an efficient terahertz emitter. In general, terahertz radiation from semiconductors is very complex since multiple emission mechanisms compete to dominate and those mechanisms are strongly dependent on the basic optical/electrical properties of semiconductors. On the other hand, from a comprehensive understanding of terahertz emission mechanism from semiconductors, we can elucidate the material properties such as carrier transport mechanisms. Due to its extremely low probability of intervalley scattering and strong intrinsic electric field, InN has received much attention in terahertz range applications.⁵⁻¹¹ Typically, as-grown InN film is unintentionally doped *n*-type and terahertz emission from the undoped InN is much weaker than that from InAs due to large screening from high intrinsic carrier density. Doping InN with proper acceptors, such as Mg, is expected to reduce the carrier density and enhance the radiation intensity. Recently, the enhanced radiation from Mg-doped InN compared to that from Si-doped InN has been reported.¹² In this letter, we report terahertz emission from a series of Mg-doped *c*-InN (InN:Mg) films with different carrier concentrations (*n*). As the carrier concentration de-

creases by Mg doping, terahertz emission increases due to the combined effects of carrier compensation and the reduced screening of the photo-Dember field. Meanwhile, for InN:Mg samples with the electron concentration below a critical value near $1 \times 10^{18} \text{ cm}^{-3}$, negative polarity of terahertz radiation was observed. Negative terahertz polarity from InN reflects the dominant contribution of drift current induced by the strong surface band bending within the space-charge layer extending over the optical absorption depth at the excitation wavelength.

For this work, a wurtzite N-polar (*-c*-axis) undoped InN film and seven Mg-doped InN films with different carrier concentrations were grown by plasma-assisted molecular beam epitaxy on Si(111) using the epitaxial AlN/ β -Si₃N₄ double-buffer layer technique. The film thicknesses of the samples are in the range of 1–1.5 μm . Mg doping was performed with a high-purity Mg(6N) Knudsen cell and the Mg doping level was controlled by regulating the cell temperature between 180 and 270 °C. The electron concentrations and electron mobilities were determined by room-temperature Hall effect measurements for Mg-doped InN films and an undoped InN film.

Time-domain terahertz emission measurements were performed using a Ti:sapphire regenerative amplifier laser system, which delivers ~ 50 fs optical pulses at a center wavelength of 800 nm with a repetition rate of 1 kHz. For this experiment, the pump laser beam is collimated on the samples with a spot size of ~ 2 mm at the incident angle of 70°. The terahertz pulses were detected by free-space electro-optic sampling in a 2-mm-thick ZnTe crystal as a function of delay time with respect to the optical pump pulse. The experimental details can be found elsewhere.⁹

It is known that photocarriers generated close to the surfaces of semiconductors can be accelerated by an appropriate electric field and the resultant transient electric dipole can lead to the generation of terahertz pulses. The electric field can be provided either externally by separated electrodes in photoconductive antennas or internally by the photo-Dember field or by the surface depletion/accumulation field. Typically, the distinction between the photo-Dember effect and surface field acceleration can be made by monitoring the polarity of terahertz wave. In wide bandgap semiconductors,

^{a)}Author to whom correspondence should be addressed. Electronic mail: hyahn@mail.nctu.edu.tw.

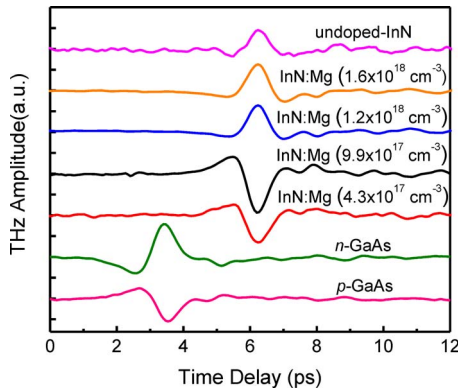


FIG. 1. (Color online) The time-domain terahertz waveforms of the as-grown (undoped) InN and Mg-doped InN films. The electron concentrations of InN:Mg films are 4.3×10^{17} , 9.9×10^{17} , 1.2×10^{18} , and $1.6 \times 10^{18} \text{ cm}^{-3}$ and that of undoped InN is $3.1 \times 10^{18} \text{ cm}^{-3}$. InN:Mg films with the electron concentration below $\sim 1 \times 10^{18} \text{ cm}^{-3}$ have a negative polarity, while others, including undoped InN film, have a positive polarity. The terahertz waveforms of *n*-type and *p*-type GaAs are shown together for comparison.

such as GaAs, Fermi level-pinning occurs in such a way to bend the bands to form a surface built-in field in the depletion region at the surface. The direction of the band bending-induced electric field for these semiconductors depends on the dopant types so that the directions of drift current are opposite for *n*-type and *p*-type GaAs and the corresponding terahertz waves show the opposite polarity. However, InN, similar to the case of InAs (Refs. 13 and 14), has the surface Fermi level located above the conduction band minimum and thus the surface band bending for both *n*-type and *p*-type InN is downward. As a result, the terahertz wave polarities of *n*-type and *p*-type InN due to the surface electric field are both negative. Recently, Lin *et al.*¹⁵ reported the observation of the negative polarity of terahertz wave from an undoped *n*-type InN excited at very low fluence below $0.6 \mu\text{J}/\text{cm}^2$, indicating that terahertz radiation is attributed to the drift current induced by the internal surface electric field. For highly excited InN, however, terahertz radiation induced by the surface electric field is overpowered by the photo-Dember field so that its polarity is positive.⁵⁻⁹

Terahertz emission due to both the photo-Dember effect and surface field acceleration depends closely on carrier concentration so that the amplitude and the polarity of terahertz waves can be determined by the competition between these emission mechanisms at a carrier concentration. In order to investigate the effect of Mg doping to terahertz emission, we measured the time-domain terahertz emission from a series of Mg-doped InN samples with different carrier concentration *n* and an undoped InN film ($n = 3.1 \times 10^{18} \text{ cm}^{-3}$) excited at the pump fluence of $\sim 200 \mu\text{J}/\text{cm}^2$. In Fig. 1, the terahertz waveforms of the selected samples are shown. The waveforms of InN:Mg samples with $n = 1.2 \times 10^{18}$ and $1.6 \times 10^{18} \text{ cm}^{-3}$ and the undoped InN have the positive polarity, while those of the samples with $n = 4.3 \times 10^{17}$ and $9.9 \times 10^{17} \text{ cm}^{-3}$ exhibit the pronounced negative polarity. The observed negative terahertz polarity is a remarkable result for *c*-InN since terahertz emission from *c*-InN at the current pump fluence is known to be dominated by the photo-Dember effect and the corresponding terahertz polarity should be positive for both *n*-type and *p*-type InN. The terahertz polarity of the sample is confirmed by comparing it to those of *n*-type and *p*-type GaAs wafers, which shows the

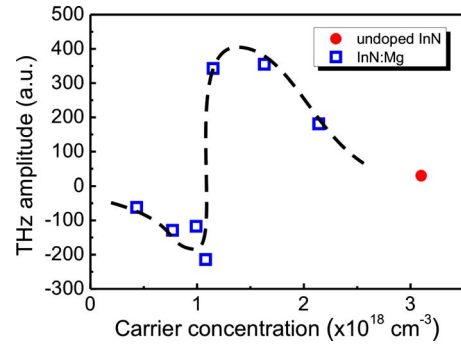


FIG. 2. (Color online) Peak terahertz amplitudes of InN:Mg (open squares) and undoped InN (solid circle) samples are plotted as a function of the electron concentration determined by room-temperature Hall measurement. Each sample was photoexcited at the pump intensity at $200 \mu\text{J}/\text{cm}^2$. The dashed line is drawn for eye guiding.

opposite signs of polarity depending on the doping type. Figure 1 shows that the observed negative polarity of InN:Mg samples are the same as that of the *p*-type GaAs, confirming that the drift current directs into the sample. Meanwhile, no significant azimuthal angle dependence of terahertz emission was measured for our samples so that we can rule out the contribution of the optical rectification effect for terahertz emission. Thus, one remaining possible explanation for the negative polarity of terahertz radiation is the dominant surface acceleration effect due to the downward surface band bending.

A recent result of terahertz emission from InN:Mg demonstrated that the carrier compensation between the concentration of native donors (n_D) and acceptors (n_A) can cause the enhancement in terahertz emission compared to that from Si-doped *n*-type InN.¹² A similar concentration-dependent enhancement in terahertz radiation is observed from our InN:Mg samples. In Fig. 2, we observe that the magnitude of terahertz radiation increases as the carrier concentration decreases from that of undoped InN film and the maximum emission occurs for samples with $n = 1.2\text{--}1.5 \times 10^{18} \text{ cm}^{-3}$ and the terahertz polarities of these samples are positive. Meanwhile, for samples with lower carrier concentrations than $\sim 1 \times 10^{18} \text{ cm}^{-3}$ (n_c), the amplitude of terahertz radiation becomes smaller with a negative polarity. We also measured the optical pump intensity dependence of terahertz radiation for samples with opposite polarities. Figure 3 shows

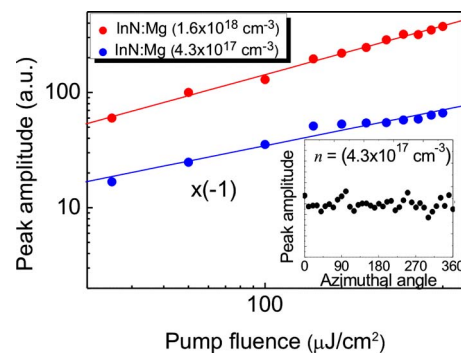


FIG. 3. (Color online) The amplitude of terahertz emission field vs. pump fluence for InN:Mg films with $n = 4.3 \times 10^{17}$ and $1.6 \times 10^{18} \text{ cm}^{-3}$. The sign of data of InN:Mg film with $n = 4.3 \times 10^{17} \text{ cm}^{-3}$ is inverted to be positive. Inset shows a typical azimuthal angle-dependent terahertz radiation from InN:Mg film.

that terahertz emission increases linearly with the pump fluence for both samples and the saturation of the emission is not observed.

Our Hall effect measurement shows that the electron concentration decreases as the Mg doping level increases. It indicates that doped Mg acceptors compensate the native donors in the unintentionally doped *n*-type InN films and reduce the electron concentration in the InN:Mg film. Therefore, in order to explain our terahertz emission data, we consider the InN:Mg films to be the carrier compensated *n*-type films with reduced electron carrier density. According to the surface field model, the highest terahertz emission and the largest depletion width ($l \propto |n_A - n_D|^{-1/2}$) occur for a highly compensated semiconductors with $n_A \approx n_D$.^{12,16} Therefore, the negative terahertz polarity observed for InN:Mg samples with $n < n_c$ indicates that the carriers in these sample are highly compensated and the large downward band bending occurs across the space-charge layer whose depth extends to cover the penetration depth ($d \sim 133$ nm)¹⁷ of the pump pulse (800 nm). And terahertz emission from these films is mainly due to the surface field acceleration effect. On the contrary, for InN:Mg samples with $n > n_c$, the space-charge layer where band bending occurs might be much shorter than d due to the partial carrier compensation and the photo-Dember effect dominates terahertz emission in the bulk region of InN:Mg.¹² In this bulk region, the reduction in screening of the photo-Dember field can be more significant as n decreases further from that of undoped InN. The maximum positive polarity terahertz emission is, therefore, obtained before the sharp increase in depletion depth occurs near n_c .

In summary, we have shown that for Mg-doped InN, a transition of dominant terahertz emission mechanism between the photo-Dember effect and surface field acceleration occurs depending on the carrier concentration. For highly compensated Mg-doped samples with the carrier concentration below the critical value, terahertz polarity is negative, indicating the significant contribution of the surface field acceleration effect and the space-charge layer could cover the

entire photoexcited region. The partially compensated Mg-doped samples generate intense terahertz radiation with positive polarity and this may be due to the enhanced photo-Dember field with reduced screening.

This work was supported by the National Science Council (Grant No. NSC 96-2112-M-009-016-MY3) and the ATU program of the Ministry of Education, Taiwan.

- ¹R. E. Jones, K. M. Yu, S. X. Li, W. Walukiewicz, J. W. Ager, E. E. Haller, H. Lu, and W. J. Schaff, *Phys. Rev. Lett.* **96**, 125505 (2006).
- ²X. Wang, S.-B. Che, Y. Ishitani, and A. Yoshikawa, *Appl. Phys. Lett.* **90**, 201913 (2007).
- ³P. D. C. King, T. D. Veal, P. H. Jefferson, and C. F. McConville, *Phys. Rev. B* **75**, 115312 (2007).
- ⁴Y. M. Chang, Y.-L. Hong, and S. Gwo, *Appl. Phys. Lett.* **93**, 131106 (2008).
- ⁵R. Ascáubi, I. Wilke, K. Denniston, H. L. Lu, and W. J. Schaff, *Appl. Phys. Lett.* **84**, 4810 (2004).
- ⁶B. Pradarutti, G. Matthäus, C. Brückner, S. Riehemann, G. Notni, S. Nolti, V. Cimalla, V. Lebedev, O. Ambacher, and A. Tünnermann, *Proc. SPIE* **6194**, 619401 (2006).
- ⁷G. D. Chern, E. D. Readinger, H. Shen, M. Wraback, C. S. Gallinat, G. Koblmüller, and J. S. Speck, *Appl. Phys. Lett.* **89**, 141115 (2006).
- ⁸X. Mu, Y. Ding, K. Wang, D. Jena, and Y. B. Zotova, *Opt. Lett.* **32**, 1423 (2007).
- ⁹H. Ahn, Y.-P. Ku, Y.-C. Wang, C.-H. Chuang, S. Gwo, and C.-L. Pan, *Appl. Phys. Lett.* **91**, 132108 (2007).
- ¹⁰H. Ahn, Y.-P. Ku, C.-H. Chuang, C.-L. Pan, H.-W. Lin, Y.-L. Hong, and S. Gwo, *Appl. Phys. Lett.* **91**, 163105 (2007).
- ¹¹H. Ahn, Y.-P. Ku, Y.-C. Wang, C.-H. Chuang, S. Gwo, and C.-L. Pan, *Appl. Phys. Lett.* **92**, 102103 (2008).
- ¹²I. Wilke, R. Ascáubi, H. Lu, and W. J. Schaff, *Appl. Phys. Lett.* **93**, 221113 (2008).
- ¹³M. Noguchi, K. Hirakawa, and T. Ikoma, *Phys. Rev. Lett.* **66**, 2243 (1991).
- ¹⁴L. Ö. Olsson, C. B. M. Andersson, M. C. Håkansson, J. Kanski, L. Ilver, and U. O. Karlsson, *Phys. Rev. Lett.* **76**, 3626 (1996).
- ¹⁵K. I. Lin, J. T. Tsai, T. S. Wang, J. S. Hwang, M. C. Chen, and G. C. Chi, *Appl. Phys. Lett.* **93**, 262102 (2008).
- ¹⁶R. Ascáubi, C. Schneider, I. Wilke, R. Pino, and P. S. Dutta, *Phys. Rev. B* **72**, 045328 (2005).
- ¹⁷H. Ahn, C.-H. Shen, C.-L. Wu, and S. Gwo, *Appl. Phys. Lett.* **86**, 201905 (2005).